

STRUCTURES OF Cl ADLAYERS ON Ag(111) SURFACE

N.V. PETROVA, I.N. YAKOVKIN, O.M. BRAUN

PACS 68.43.Bc; 68.43.Fg
©2011Institute of Physics, Nat. Acad. of Sci. of Ukraine
(46, Nauky Ave., Kyiv 03680, Ukraine)

The lateral interaction between chlorine atoms adsorbed on the Ag(111) surface results in the formation of a $(\sqrt{3}\times\sqrt{3})R30^\circ$ structure at the coverage $\theta = 0.33$. This structure is experimentally observed by the methods of low-energy electron diffraction and scanning tunnel microscopy at sufficiently low substrate temperatures. With increase in the temperature, the $(\sqrt{3}\times\sqrt{3})R30^\circ$ structure disorders, which results in the vanishing of the characteristic reflections from the diffraction image at room temperature. The Monte Carlo simulation with parameters of the lateral interaction energy calculated with the help of the density functional theory has elucidated important features of the formation of surface structures and the order-disorder transition taking place with increase in the temperature. In particular, it is shown that the transition is very abrupt, which is due to a sufficient number of free adsorption sites and the substantial repulsive lateral interaction between adatoms.

1. Introduction

The urgency of a detailed investigation of the properties of chlorine adlayers on the silver surface is dictated, first of all, by demands of catalysis. Chlorine is a selectivity promoter of the reaction of ethylene oxidation on the catalytic silver surface used in the chemical industry. The adsorption of chlorine on Ag(111) was widely studied both theoretically and experimentally [1–21], particularly with the help of the methods of low-energy electron diffraction (LEED) [1–5], surface-extended X-ray absorption fine structure (SEXAFS) [5, 14], thermal desorption [2,3], Auger spectroscopy [1–3], scanning tunnel microscopy (STM) [4, 13, 15], temperature programmed X-ray photoelectron spectroscopy (TPXPS), as well as with the use of calculations performed in the framework of the density functional theory (DFT) [17–21].

The adsorption of chlorine on the Ag(111) surface is accompanied by the dissociation of a Cl_2 molecule (exothermic reaction with almost zero activation barrier [2]). The initial sticking coefficient of Cl on the Ag(111) surface amounts to 0.4 [3]. At room temperature and coverages up to a half of a monolayer (ML), chlorine does not diffuse into the substrate, and its atoms remain in the chemisorbed state on the surface [16, 21]. At

low coverages, the bond between chlorine atoms and the Ag(111) surface is rather strong (2.9–3.0 eV for $\theta = 0.33$ ML in the $(\sqrt{3}\times\sqrt{3})R30^\circ$ structure [17]), and its energy exceeds the dissociation energy of a chlorine molecule (2.476 eV [21]). According to the rule proposed in [2, 22] for diatomic gases, such a relation between the binding energies testifies to the fact that, at low coverages (up to 0.33 ML), chlorine will be desorbed in the atomic form (i.e. without recombination into Cl_2). The atomic form of the chlorine desorption from the Ag(111) surface was really observed in [2]. At coverages close to the saturation one, the desorption takes place in the form of AgCl [3, 12].

For larger coverages ($\theta > 0.5$) and temperatures in the range 300–600 K, the Ag(111) surface is reconstructed with the formation of assemblies of triangular islands with the (3×3) symmetry [13] surrounded by a film with the $(\sqrt{3}\times\sqrt{3})R30^\circ$ structure. At the formation of the saturated chlorine coverage, Ag_3Cl_7 clusters are generated at the boundaries between islands of the (3×3) structure. The maximum possible coverage corresponds to 0.55. With increase in the temperature, chlorine is desorbed at temperatures of 650–780 K in the form of silver chloride clusters [3, 16].

The LEED studies of chlorine on the Ag(111) surface performed at room temperature [1–5] did not reveal the formation of ordered structures at low coverages. A well-ordered structure is observed only for coverages somewhat lower than the saturation one. It is worth noting that there is no consensus in the literature as regards both the periodicity of the structures observed under saturation conditions and the coverage corresponding to this state. At low temperatures, however, chlorine atoms form a well-ordered $(\sqrt{3}\times\sqrt{3})R30^\circ$ structure on the Ag(111) surface at $\theta = 0.33$ [5] (Fig. 1, *a*), and, as follows from DFT calculations [19, 21], a hexagonal honeycomb structure can be formed at $\theta = 0.5$ (Fig. 1, *b*).

In [5], the LEED method was used for studying the formation of the $(\sqrt{3}\times\sqrt{3})R30^\circ$ structure of chlorine on the Ag(111) surface depending on the temperature. A sharp LEED image observed at low temperatures testifies to the formation of a well-ordered $(\sqrt{3}\times\sqrt{3})R30^\circ$ structure.

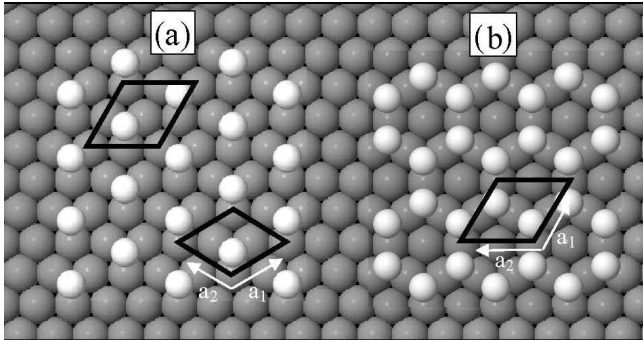


Fig. 1. Models of the $(\sqrt{3}\times\sqrt{3})R30^\circ$ (a) and hexagonal honeycomb (b) structures of Cl on the Ag(111) surface. The rhombs mark the unit cells used in the DFT calculations

However, after reaching a temperature of 195 K, the reflections suddenly become diffuse, which is an evidence of its disorder. The experimentally observed order-disorder transition is very abrupt (the transition temperature corresponds to the temperature interval ~ 2 K).

The present work studies the lateral interaction in chlorine layers adsorbed on the Ag(111) surface at low coverages (up to 0.5 ML), where the diffusion of chlorine into the bulk can be neglected. Particularly, the formation of Cl structures on the Ag(111) surface and the order-disorder transition at various temperatures and coverages are simulated by the Monte Carlo technique with the use of parameters of the lateral interaction estimated from DFT calculations performed for various distances between adatoms.

2. Procedure

The lateral interaction energy was calculated in the framework of the density functional theory with the help of the ABINIT software [23] using norm-conserving pseudopotentials [24] and the gradient approximation for the exchange-correlation potential [25]. The calculations for the surface were performed in the framework of the model of repetitive layers with chlorine atoms adsorbed from one side of the layer. The layer thickness consisted of four atomic planes of Ag(111), chlorine atoms adsorbed from one side, and a vacuum gap approximately 10 Å in thickness. The lateral interaction between Cl adatoms on the Ag(111) surface was calculated with the use of a (3×3) surface unit cell.

The positions of chlorine adatoms and two upper layers of the Ag(111) surface were optimized until forces acting on atoms were larger than 0.03 eV/Å. The efficiency of a division of the Brillouin zone was checked using various lattices for k -points to reach the convergence

of 0.01 eV with respect to the total energy and 0.01 Å with respect to the atomic positions. For the Ag(111) surface, a set of $3\times 3\times 1$ special k -points [27] appeared sufficient. All calculations were carried out using a cut-off energy of 30 Hartree.

Before the adsorption of Cl atoms, the positions of atoms forming the substrate were optimized so as to minimize the total energy of the system. As a result, the interatomic distance for the upper Ag layer decreased by $\sim 5\%$ as compared to the distance in the bulk of a silver crystal (the lattice constant for a bulk silver crystal was estimated as 4.27 Å in accordance with previous calculations [19] providing the value of 4.16 Å). For the second and third layers, only an insignificant shift is observed. The optimization of the positions of chlorine adatoms together with the silver surface layer gives rise to the back relaxation of the Ag(111) surface.

To estimate the binding (adsorption) energy between a chlorine atom and the Ag(111) surface, we calculated the total energy for the $(\sqrt{3}\times\sqrt{3})R30^\circ$, 2×2 , and honeycomb structures on the 4-layer Ag(111) substrate. The binding energy E_b (positive) between a chlorine atom and the Ag(111) surface calculated per one chlorine atom amounts to

$$E_b = -(E_{\text{Ag+Cl}} - E_{\text{Ag}} - nE_{\text{Cl}})/n,$$

where $E_{\text{Ag+Cl}}$ is the total energy of the system with n adsorbed chlorine atoms in the surface cell, while E_{Ag} and E_{Cl} are the total energies of the substrate and a chlorine atom, respectively.

The Monte Carlo simulations of the formation of chlorine structures on the Ag(111) surface were carried out using the developed programs checked by simulating various adsorption systems [22, 28, 29]. This method applies the standard Metropolis algorithm in the lattice gas model with regard for the long-range lateral interaction between particles adsorbed on the Ag(111) surface presented by a lattice of 60×36 adsorption sites with the periodic boundary conditions.

The particle ordering was performed by shifting a randomly chosen adatom to the neighboring adsorption site with regard for the existence of a diffusion barrier. The probability of such a transition, $\exp(-\Delta E/kT)$, is determined by the difference ΔE between the energies of lateral interaction with other adsorbed atoms for the initial and final configurations. If a shift to the neighboring adsorption site results in a gain of the energy of the system ($\Delta E < 0$) or the transition probability considerably exceeds a standard random number, then this shift is realized. Otherwise, the particle remains at the initial site.

The relative intensities of the LEED reflections were estimated in the kinematic approximation:

$$I(h, k) = |\Sigma_n \exp\{2\pi i(hx_n + ky_n)\}|^2,$$

where the summation was performed over the occupied adsorption sites with the coordinates x_n and y_n . The intensity distribution of LEED reflections was obtained for various coordinates in the reciprocal space h and k . The corresponding reflections were presented by a circle, whose diameter corresponded to their relative intensity.

3. Results

The performed calculations of the total energy demonstrate that, for chlorine atoms on the Ag(111) surface, threefold adsorption sites are the most advantageous with respect to other possible positions. Figure 1 presents the models of the $(\sqrt{3}\times\sqrt{3})R30^\circ$ and hexagonal honeycomb structures of chlorine on the Ag(111) surface and the corresponding unit cells used in the DFT calculations. According to other DFT calculations [17], the binding energy of a chlorine adatom located at a threefold site for the $(\sqrt{3}\times\sqrt{3})R30^\circ$ structure (Fig. 1, *a*) amounts to 2.80 eV, which is 0.1 eV higher than the binding energy of Cl in a bridge position. The adsorption in on-top positions of silver atoms is unstable. The energy difference between fcc and hcp threefold adsorption sites is less than 0.01 eV, which is within the estimated calculation error. Thus, at low coverages, chlorine atoms occupy fcc and hcp threefold sites with the distance of the Cl–Ag bond equal to 2.66 Å, which agrees with the previously estimated values of 2.48 Å [5], 2.62 Å [17], and 2.7 Å [14, 21]. An increase of the coverage is accompanied by a reduction of the chemisorption energy, which is due to the repulsive lateral interaction between chlorine adatoms (Table 1).

The relative diameters of Cl and Ag atoms can be estimated from the calculated distance of the Cl–Ag bond (2.66 Å) and the distance between silver atoms forming a periodic hexagonal structure of Ag(111) (2.89 Å). Particularly, the radius of the tangent Ag spheres can be

Table 1. Binding energies E_b (eV) of an oxygen atom on the Ag(111) surface at various coverages (d (Å) is the interatomic distance in the structure)

θ	Structure	d (Å)	E_b
1.00	(1×1)	2.89	1.67
0.50	(2×2)	3.34	2.72
0.33	$(\sqrt{3}\times\sqrt{3})R30^\circ$	5.01	2.80
0.25	(2×2)	5.78	3.11

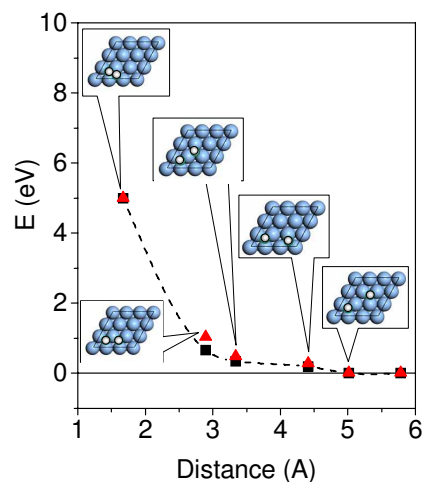


Fig. 2. Lateral interaction energies for various distances between chlorine adatoms. The results of DFT calculations are marked by squares connected by the dotted line. Triangles mark the parameters of MC simulations

estimated as 1.45 Å, while the radius of a chlorine atom in the $(\sqrt{3}\times\sqrt{3})R30^\circ$ structure is equal to 1.21 Å. Thus, the size of an adsorbed chlorine atom somewhat exceeds the bond distance in a free Cl₂ molecule, which is caused by the existence of some negative charge acquired by the chlorine atom due to the adsorption. So, the ratio of the radii of Cl and Ag atoms determined as r_{Cl}/r_{Ag} amounts to 0.83 (this ratio was used for depicting atomic spheres in Fig. 1).

In order to perform the Monte Carlo simulations of the formation of ordered Cl structures on the Ag(111) surface, it is necessary to determine parameters of the lateral interaction for various distances between adatoms (Table 1). For five first neighbors, the distances between chlorine atoms located at threefold sites amount to 1.67, 2.89, 3.34, 4.41, 5.01, and 5.78 Å, respectively (see the inset in Fig. 2). It is worth noting that the distance between atoms located in the nearest neighboring threefold adsorption sites is lower than the distance between chlorine atoms in a free molecule (2.0 Å), which results in a considerable repulsive interaction between chlorine adatoms, making impossible their arrangement of such a kind. In this case, the optimization of the atomic positions performed without additional restrictions results in that the atoms inevitably leave threefold sites, which complicates the estimation of the lateral interaction energy. A similar problem also arises for the second and third neighbors due to the significant lateral repulsion between Cl atoms at such distances. Due to this fact, the lateral interaction at such distances was

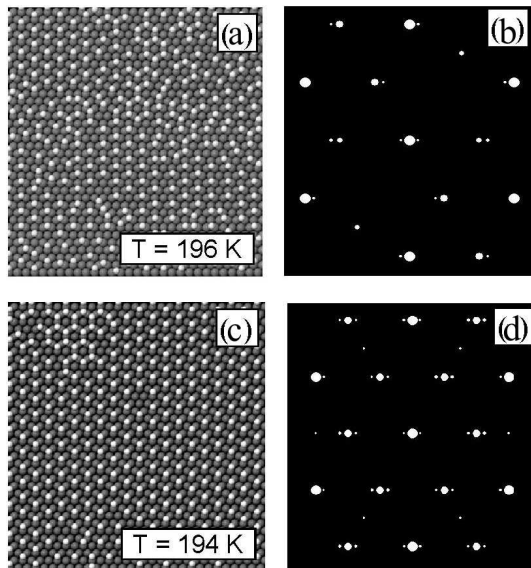


Fig. 3. Monte Carlo simulation of the formation of the $(\sqrt{3}\times\sqrt{3})R30^\circ$ ordered structure of Cl at the coverage $\theta = 0.33$: domains of the $(\sqrt{3}\times\sqrt{3})R30^\circ$ structure ($T = 196$ K) (a), diffraction image with split and extinguished reflections (b), $(\sqrt{3}\times\sqrt{3})R30^\circ$ ordered structure ($T = 194$ K) (c), and sharp diffraction image (d)

estimated with fixed coordinates and the distance from the substrate typical of the $(\sqrt{3}\times\sqrt{3})R30^\circ$ structure.

The estimated energies of the lateral interaction between chlorine adatoms as functions of the interatomic distance are presented in Fig. 2, a and Table 2. The lateral repulsion between adsorbed atoms at large distances can be explained by the presence of the dipole-dipole interaction. However, the dipole moment of a chlorine atom adsorbed on the silver surface estimated from the initial slope of the coverage dependence of the work function [30] amounts to only 0.75–0.9 D. For distances corresponding to the second and third neighbors, the dipole-dipole interaction appears too weak and cannot explain the significant repulsion arising between chlorine atoms (see Fig. 2).

Thus, the lateral interaction has a complex nature and can be probably related to the indirect interaction between adsorbed chlorine atoms [31]. The Monte Carlo simulation using the calculated lateral interaction energies provides a good description of the formation of the $(\sqrt{3}\times\sqrt{3})R30^\circ$ structure at $\theta = 0.33$. However, the temperature of the order-disorder transition for this structure appears lower than that observed experimentally [5], which can be caused by the mentioned difficulties in the calculation of the lateral interaction at small distances. To obtain the right value of the temperature of

the order-disorder transition, the parameters of the lateral interaction for the distances corresponding to the second and third neighbors were somewhat increased (see Table 2).

At the coverage $\theta = 0.33$, the ordering of a chlorine monolayer was simulated by gradually decreasing the temperature. The number of diffusion MC steps at each temperature was sufficient to reach the equilibrium. The same way as in the experiment [1–5], the chlorine film is disordered at small coverages and the temperature $T = 210$ K, so the diffraction image has no reflections. At a temperature of 196 K, the structure $(\sqrt{3}\times\sqrt{3})R30^\circ$ starts to form, but the presence of domain walls results in the splitting of the reflections and a decrease of their intensity (Fig. 3, a, b). As the temperature falls to $T = 194$ K, the film suddenly becomes well-ordered (Fig. 3, c) and demonstrates a sharp diffraction image (Fig. 3, d). The further decrease of the temperature does not lead to any changes in the film structure.

It is worth noting that the formation of the $(\sqrt{3}\times\sqrt{3})R30^\circ$ structure at $\theta = 0.33$ is accompanied by the generation of fragments of the honeycomb structure, which results in the appearance of reflections typical of the (2×2) structure (Fig. 3, b). This structure is evidently formed due to a random local increase of the concentration that exceeds the stoichiometric one (0.33) for the $(\sqrt{3}\times\sqrt{3})R30^\circ$ structure. A small skeleton of this structure is observed even at the temperature $T = 194$ K, when the formation of the $(\sqrt{3}\times\sqrt{3})R30^\circ$ structure is practically completed (Fig. 3, c).

The process of surface diffusion can be considered as successive jumps of chlorine atoms from one threefold site to another one with overcoming the activation barrier. The height of this barrier corresponds to the difference between the energies of a chlorine atom at a threefold site and at a bridge one (according to DFT calculations, this difference amounts to ~ 0.1 eV). Due to the limited (owing to the diffusion barrier) mobility

Table 2. Lateral interaction energies (eV) obtained from DFT calculations and parameters of the Monte Carlo simulation

Neighbors	Distance between atoms (Å)	E_{int} (eV) DTF	E_{int} (eV) MC
1-st	1.67	5.00	5.00
2-nd	2.89	0.72	1.03
3-rd	3.34	0.40	0.47
4-th	4.41	0.25	0.28
5-th	5.01	0.05	0.02
6-th	5.78	0	0

of adatoms on the surface, the degree of order of the obtained structures considerably depends on the rate of decrease of the temperature. In particular, if this rate is high, the restriction of the mobility results in the formation of separate domains of the $(\sqrt{3}\times\sqrt{3})R30^\circ$ structure. In this case, the diffusion image demonstrates reflections with characteristic weak satellites, which testifies to the splitting of beams due to the phase shift for electrons scattered by different domains. Respectively, the intensity of reflections characteristic of the $(\sqrt{3}\times\sqrt{3})R30^\circ$ structure significantly decreases. As a result, the abruptness of the order-disorder transition depends on the rate of decrease of the temperature (see Fig. 4). At the parameters of the lateral interaction listed in Table 2, the order-disorder transition takes place in a very narrow temperature interval (~ 2 K), which agrees with experimental observations.

The diameter of a chlorine atom estimated from the distance of the Cl–Ag bond in the $(\sqrt{3}\times\sqrt{3})R30^\circ$ structure amounts to 2.4 Å, whereas the lattice spacing on the Ag(111) surface is equal to 2.89 Å. Due to the relatively small radius of a chlorine atom, they could form, in principle, even a full (1×1) monolayer. That is why the limiting coverage is close to 0.5 ML, which is due to the considerable repulsive lateral interaction that significantly decreases the effective adsorption energy, rather than to the large dimensions of chlorine atoms. This fact is also confirmed by two peculiarities of this system: 1. At high temperatures and a large exposure, chlorine atoms diffuse into the substrate, which would be impossible if they were larger than silver ones; 2. The abruptness of the order-disorder transition for the $(\sqrt{3}\times\sqrt{3})R30^\circ$ structure testifies to the existence of a sufficient space for the two-dimensional evaporation of Cl adatoms (we recall that, in the case of dense structures formed close to the saturation point, a smooth transition is observed with increase in the temperature). Indeed, in the process of ordering, chlorine atoms inevitably appear at the distance corresponding to the lattice spacing of the Ag(111) surface (2.89 Å).

DFT calculations [19, 21] have demonstrated that, at the chlorine coverage on the Ag(111) surface $\theta = 0.5$, the most profitable structure is the hexagonal honeycomb one (Fig. 1, *b*). However, the formation of this structure was not observed in LEED experiments. This fact was related to a large size of chlorine atoms and the possibility of the formation of only incommensurable hexagonal structures (10×10) [2], (13×13) [5], or (17×17) [4] at such a coverage. However, the repulsion between Cl adatoms for the distances typical of the honeycomb (2×2) structure (corresponding to the third

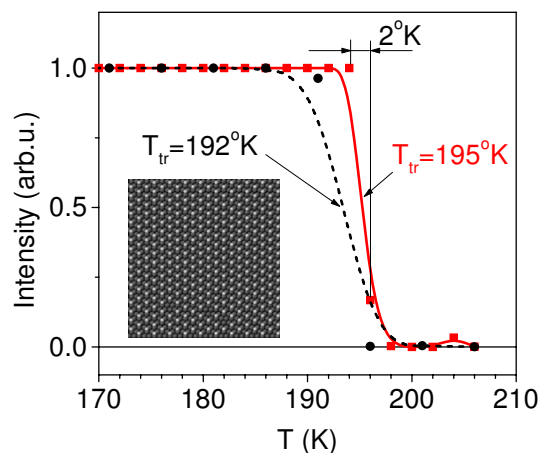


Fig. 4. Diagram of the order-disorder transition for the $(\sqrt{3}\times\sqrt{3})R30^\circ$ structure at $\theta = 0.33$. The abruptness of the transition depends on the cooling rate (solid line corresponds to MC simulations performed at a temperature step of 2 K, dotted line – 5 K)

nearest neighbors, see Fig. 2) is inessential to make the formation of such a structure impossible.

At the coverage $\theta = 0.5$, the Monte Carlo simulations of the Cl ordering were performed for the same parameters of the lateral interaction as for the $(\sqrt{3}\times\sqrt{3})R30^\circ$ structure with a gradual decrease in the temperature. At room temperature, the film is disordered; elements of the honeycomb structure are formed, as the temperature falls to 200 K, whereas at $T \approx 160$ K, domains of the honeycomb structure occupy the whole surface. However, the expected (2×2) diffraction structure is not formed due to the phase shifts at the electron scattering by different domains separated from one another by domain walls, which results in the vanishing of the LEED reflections typical of the (2×2) structure.

4. Conclusions

We have studied the lateral interaction between chlorine atoms adsorbed on the Ag(111) surface at low coverages (up to 0.5 ML), at which the diffusion of chlorine into the bulk can be neglected. The parameters of the lateral interaction energy for various distances between adsorbed chlorine atoms were obtained from the calculations performed in the framework of the density functional theory. The formation of the $(\sqrt{3}\times\sqrt{3})R30^\circ$ structure at $\theta = 0.33$ and the honeycomb structure at $\theta = 0.5$ is reproduced by Monte Carlo simulations. It is shown that the order-disorder transition for the $(\sqrt{3}\times\sqrt{3})R30^\circ$ structure is very abrupt, which is explained by a suffi-

cient number of free adsorption sites for this structure at the considerable repulsive interaction between adatoms.

The diffusion barrier with a height of 0.1 eV estimated from the difference between the chemisorption energies of a threefold site and a bridge position results in a restriction of the atomic mobility, which is essential for the formation of ordered structures. In the case where a film consists of domains of the ordered structure, the diffraction image contains the characteristic splitting of reflections (for the $(\sqrt{3}\times\sqrt{3})R30^\circ$ structure), which is accompanied by a decrease of their intensity or results in the vanishing of the corresponding reflections in the case of a large number of domains (for the honeycomb (2×2) structure).

We thank B.V. Andryushechkin and K.N. Eltsov for useful advices. The work was partially performed in the framework of the Ukrainian-Russian Grant NANU-RFBR No. RFBR/3-10-26.

1. G. Rovida and F. Pratesi, *Surf. Sci.* **51**, 270 (1975).
2. P.J. Goddard and R.M. Lambert, *Surf. Sci.* **67**, 180 (1977).
3. M. Bowker and K.C. Waugh, *Surf. Sci.* **134**, 639 (1983).
4. B.V. Andryushechkin, K.N. Eltsov, V.M. Shevlyuga, and V.Yu. Yurov, *Surf. Sci.* **407**, L633 (1998).
5. A.G. Shard and V. R. Dhanak, *J. Phys. Chem. B* **104**, 2743 (2000).
6. C.T. Campbell and M.T. Paffett, *Appl. Surf. Sci.* **19**, 28 (1984).
7. R.A. Marbrow and R.M. Lambert, *Surf. Sci.* **71**, 107 (1978).
8. Y.Y. Tu and J.M. Blakely, *Surf. Sci.* **85**, 276 (1979).
9. M. Kitson and R.M. Lambert, *Surf. Sci.* **100**, 368 (1980).
10. M. Bowker, K.C. Waugh, B. Wolfendale, G. Lamble, and D.A. King, *Surf. Sci.* **179**, 254 (1987).
11. B.V. Andryushechkin, K.N. Eltsov, V.M. Shevlyuga, and V.Yu. Yurov, *Surf. Sci.* **433-435**, 109 (1999).
12. B.V. Andryushechkin, K.N. Eltsov, V.M. Shevlyuga, and V.Yu. Yurov, *Surf. Sci.* **431**, 96 (1999).
13. B.V. Andryushechkin, V.V. Cherkez, E.V. Gladchenko, G.M. Zhidomirov, B. Kierren, Y. Fagot-Revurat, D. Malterre, and K.N. Eltsov, *Phys. Rev. B* **81**, 205434 (2010).
14. G.M. Lamble, R.S. Brooks, S. Ferrer, D.A. King, and D. Norman, *Phys. Rev. B* **34**, 2975 (1986).
15. J.H. Schott and H.S. White, *J. Phys. Chem.* **98**, 291 (1994).
16. H. Piao, K. Adib, and M.A. Barteau, *Surf. Sci.* **557**, 13 (2004).
17. K. Doll and N.M. Harrison, *Phys. Rev. B* **63**, 165410 (2001).
18. Y. Wang, Q. Sun, K.N. Fan, and J.F. Deng, *Chem. Phys. Lett.* **334**, 411 (2001).
19. N.H. de Leeuw, C.J. Nelson, C.R.A. Catlow, P. Sautet, and W. Dong, *Phys. Rev. B* **69**, 045419 (2004).
20. A. Migani and F. Illas, *J. Phys. Chem. B* **110**, 11894 (2006).
21. P. Gava, A. Kokalj, S. de Gironcoli, and S. Baroni, *Phys. Rev. B* **78**, 165419 (2008).
22. N.V. Petrova and I.N. Yakovkin, *Phys. Rev. B* **76**, 205401 (2007).
23. X. Gonze, J.-M. Beuken, R. Caracas, F. Detraux, M. Fuchs, G.-M. Rignanese, L. Sindic, M. Verstraete, G. Zerah, F. Jollet, M. Torrent, A. Roy, M. Mikami, Ph. Ghosez, J.-Y. Raty, and D.C. Allan, *Comput. Mat. Sci.* **25**, 478 (2002).
24. N. Troullier and J.L. Martins, *Phys. Rev. B* **43**, 1993 (1991).
25. J.P. Perdew, K. Burke, and M. Ernzerhof, *Phys. Rev. Lett.* **77**, 3865 (1996).
26. B.G. Pfrommer, M.Cote, S.G. Louie, and M.L. Cohen, *J. Comput. Phys.* **131**, 133 (1997).
27. H.J. Monkhorst and J.D. Pack, *Phys. Rev. B* **13**, 5188 (1976).
28. N.V. Petrova, I.N. Yakovkin, and Yu.G. Ptushinskii, *Eur. Phys. J. B* **38**, 525 (2004).
29. N.V. Petrova and I.N. Yakovkin, *Surf. Sci.* **578/1-3**, 162 (2005).
30. K. Wu, D. Wang, J. Deng, X. Wei, Y. Cao, M. Zei, R. Zhai, and Z. Gao, *Surf. Sci.* **264**, 249 (1992).
31. O.M. Braun and V.K. Medvedev, *Sov. Phys. Usp.* **32**, 328 (1989).

Received 24.12.10.

Translated from Ukrainian by H.G. Kalyuzhna

СТРУКТУРИ АДСОРБОВАНИХ ШАРІВ СІ НА ПОВЕРХНІ Ag (111)

Н.В. Петрова, І.М. Яковкін, О.М. Браун

Резюме

Наявність латеральної взаємодії між адсорбованими на поверхні Ag(111) атомами хлору приводить до формування структури $(\sqrt{3}\times\sqrt{3})R30^\circ$ при ступені покриття 0,33. Ця структура спостерігається експериментально методом дифракції повільних електронів та СТМ за умови достатньо низької температури підкладки. При збільшенні температури відбувається розупорядкування структури, внаслідок чого при кімнатній температурі дифракційна картинка вже не містить характерних рефлексів. Моделювання методом Монте-Карло з використанням

параметрів енергії латеральної взаємодії, розрахованих за допомогою методу теорії функціоналу електронної густини, дозволило з'ясувати важливі особливості формування поверхневих структур та переходу порядок-непорядок, що відбувається

з ростом температури. Показано, зокрема, що перехід є дуже різким, що пояснюється достатньою кількістю вільних адсорбційних центрів для цієї структури при суттєвій відштовхувальній взаємодії між адатомами.